Applied Clay Science 50 (2010) 342–347

Contents lists available at ScienceDirect

Applied Clay Science

journal homepage: www.elsevier.com/locate/clay

Effect of pressure on kaolinite illitization

Marco Mantovani [a], Alberto Escudero [b], Ana Isabel Becerro [a,*]

[a] Instituto de Ciencia de Materiales de Sevilla-Dpto. Química Inorgánica (CSIC-US) 41092 Sevilla, Spain
[b] Bayerisches Geoinstitut, Universität Bayreuth, 95440 Bayreuth, Germany

ARTICLE INFO

Article history:
Received 20 May 2010
Received in revised form 24 August 2010
Accepted 28 August 2010
Available online 15 September 2010

Keywords:
Muscovite/illite
Kaolinite
Hydrothermal reaction
XRD
K–F zeolite
MAS NMR

ABSTRACT

The illitization of kaolinite at increasing pressures was followed by hydrothermal experiments of kaolinite in KOH solution at 300 °C for 12 h and pressures between 500 and 3000 bar. XRD indicated a direct transformation of kaolinite into muscovite/illite with increasing pressure. However, the ^{27}Al MAS NMR spectra showed, in addition to the muscovite/illite resonances, the presence of a signal at 61 ppm that should correspond to a secondary phase, not detected by XRD. A second series of experiments at 300 °C and 1000 bar for 1, 3 and 6 h was carried out to show direct evidence of such phase. The XRD patterns of the products clearly showed the crystallization of K–F zeolite, while the ^{27}Al MAS NMR spectra of these samples displayed a signal at 61 ppm that must correspond, therefore, to Al in the K–F zeolite structure. In conclusion, kaolinite transformed into muscovite/illite when submitted to hydrothermal reaction in KOH solution with increasing pressure, with the formation of a secondary metastable phase called K–F zeolite, whose coherent diffraction domains were too small as to be detected by XRD.

1. Introduction

When sandstones and mudstones are buried, diagenetic mineral transformations occur in response to the increased temperatures and pressures. In an average typical marine mudstone, detrital kaolinite comprises ~25% of these rocks at low temperatures. An important fate of this kaolinite is its transformation to illite and eventually to phengite (Kisch, 1983). Studies of the paragenesis of authigenic illite in arkosis sandstones of various regions and ages have revealed that the illitization of kaolinite is an important reaction accounting for authigenic illite formation in sandstones during burial diagenesis (Dutta and Suttner, 1986; Hancock and Taylor, 1978; Seeman, 1979; Sommer, 1978); Martín-Martín et al., 2006)). Direct precipitation of illitic minerals from kaolin precursor has been also described in shallow-buried sandstone units from the Norwegian Continental Shelf (De Almeida, 1999).

Since Velde (1965) synthesized muscovite from kaolinite and KOH solutions, experimental illitization of kaolinite in aqueous solutions containing K^+ has been a subject of study for a number of years. Most of the studies report the influence of different factors like pH, temperature and rock/fluid ratio on the kinetics of kaolinite illitization. Chermak and Rimstidt (1990) experimentally determined the transformation rate of kaolinite to muscovite/illite in KCl solutions at temperatures of 250–307 °C, while Huang (1993) studied the conversion rate of kaolinite to muscovite/illite in KOH solution from 225 °C to 350 °C and 500 bar pressure. Bauer et al., (1998) also studied the transformation of kaolinite in high molar (0.1 to 4.0 M) KOH solutions but they applied low temperatures (35 and 80 °C). The sequence of reaction products observed under these conditions was: illite followed by KI-zeolite, phillipsite and K-feldspar. Bentabol and co-workers (Bentabol et al., 2003a; Bentabol et al., 2003b; Bentabol et al., 2006) described the results of kaolinite illitization in solutions containing NaOH, KOH and $MgCl_2$. The presence of Na^+ ions caused the formation of analcime (zeolite) at the intermediate stages of the reaction, while the presence of Mg^{2+} ions yielded thin illite particles covered by 14-Å clinochlore-like layers in addition to analcime and K-zeolite.

Most of the studies described previously used autoclaves or hydrothermal reactors that generate an internal pressure corresponding to the water vapour pressure at each temperature. The use of this type of reactors, therefore, hinders carrying out the experiments at higher pressures when working below the critical temperature of water (374 °C). To our knowledge, the only study of kaolinite illitization carried out at higher pressures was that of Huang (1993) commented previously, where direct conversion of kaolinite to muscovite/illite was observed.

Studying the transformation of kaolinite into illite with an increasing pressure is important because the formation of illite via illitization of kaolinite takes place at an intermediate burial depth of 3–4 km, where pressure can reach values of some 100 MPa (~1000 bar) (Bjorlikke, 1980). Our study was devoted to the analysis of the illitization of kaolinite in KOH solution at increasing pressures,

* Corresponding author. Postal address: c/Américo Vespucio, 49, 41092 Seville (Spain). Tel.: +34 954489545; fax: +34 954460665.
E-mail addresses: Marco.mantovani@yahoo.it (M. Mantovani), Alberto.Escudero@uni-bayreuth.de (A. Escudero), anieto@icmse.csic.es (A.I. Becerro).

0169-1317/$ – see front matter © 2010 Elsevier B.V. All rights reserved.
doi:10.1016/j.clay.2010.08.024

using the capabilities of the hydrothermal laboratory at the Bayerisches Geoinstitut (Bayreuth, Germany).

2. Methods

2.1. Hydrothermal reactions

KGa-1b kaolinite (Pruett and Harold, 1993), with the formula $(Si_{3.83}\ Al_{0.17})\ (Al_{3.86}\ Fe_{0.02}Ti_{0.11})\ (Ca, Na, K, Mg)_{0.05}\ O_{10}(OH)_8$ was supplied by the Source Clays Repository of The Clay Minerals Society (www.clays.org). A small amount of anatase appears as impurity. Each sample was prepared by placing approximately 100 mg of as received kaolinite into a gold capsule (30 mm length, 5 mm o.d., 4 mm i.d.) containing 100 μL of KOH solution (2.85 M). The gold capsules were welded shut and weighed before and after hydrothermal reaction to detect leakage during the run. Samples that leaked were discarded. The gold capsules were also flattened after welding to eliminate free space within the experimental volume. The hydrothermal experiments were conducted using a stainless-steel hydrothermal reactor in horizontal resistance furnaces equipped with thermocouple. Temperatures and times were maintained constant: 12 h and 300 °C respectively, while pressure was varied from 500 to 3000 bar. A second series of experiments were carried out at 300 °C and 1000 bar changing duration of the reaction (1, 3 and 6 h). After the hydrothermal reaction the sample was washed with distilled water, filtered and dried at room temperature. The high rock/fluid ratio used here (1000 mg/mL) yielded a moist powder that did not allow separating the solid from the liquid phase. Therefore, no chemical data of the solutions can be reported.

2.2. Characterization techniques

X-ray diffraction (XRD) patterns were recorded using a PANalytical X'Pert Pro diffractometer with Ni-filtered CuKα radiation, steps of 0.02º, and counting time of 160 s. Magic angle spinning nuclear magnetic resonance (MAS NMR) spectra were recorded in a Bruker DRX400 (9.39 T) spectrometer equipped with a multinuclear probe, using 4 mm zirconium rotors spinning at 10 kHz. ^{29}Si MAS NMR single pulse experiments were carried out with a pulse length of 2.5 μs (π/2 pulse length = 7.5 μs), an observation frequency of 79.49 MHz, and an optimized delay time of 40 s. The chemical shifts were related to tetramethylsilane. A modified version of the Bruker Winfit program, which handles the finite spinning speed in MAS experiments (Massiot et al., 2002), was used for the modelling of the ^{29}Si MAS NMR spectra. Single pulse ^{27}Al MAS NMR spectra were recorded at 104.26 MHz with a pulse length of 1.1 μs (π/2 pulse length = 11 μs) and a delay time of 0.5 s. The chemical shifts were reported in ppm from a 0.1 M $AlCl_3$ solution. Scanning electron microscopy (SEM) studies were carried out using a SEM-FEG microscope with a field emission gun operating normally at 20 kV acceleration voltage. The microscope was equipped with a XFlash Detector 4010 (Bruker AXS) for Energy Dispersive X-ray analysis.

3. Results and discussion

3.1. Phase transformations as seen by X-ray diffraction (XRD)

The XRD patterns of kaolinite before and after the hydrothermal reaction at 300 °C for 12 h at increasing pressures are shown in Fig. 1. The position of the d_{001} reflection in the starting kaolinite indicated a basal spacing of 7.14 Å, while the d value of the 060 reflection was 1.488 Å, in good agreement with the dioctahedral nature of the sample (Grim, 1968). The XRD pattern of the product obtained at 500 bar showed, in addition to the kaolinite reflections, a new set of reflections that indicated the crystallization of muscovite/illite (ICDD-PDF 29-1496 for 1*M* illite, and ICDD-PDF 07-0025 for 1*M* muscovite). In the pure $K_2O/Al_2O_3/SiO_2/H_2O$ system, as is the present case,

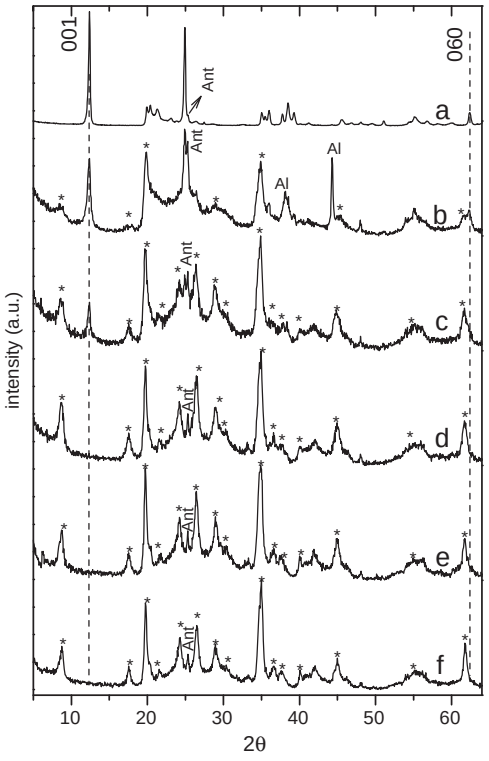

Fig. 1. XRD patterns of kaolinite before (a) and after hydrothermal reaction in 2.85 M KOH solution at 300 °C and 500 bar (b), 1000 bar (c), 1500 bar (d), 2000 bar (e) and 3000 bar (f). *: Reflections from muscovite/illite. Al: aluminium reflections of the sample holder. Ant: Anatase impurity.

muscovite and illite are indistinguishable and are grouped as muscovite/illite (Bailey, 1984). The position of the weak 001 reflection indicated a basal spacing of ~10.2 Å, characteristic of TOT layers with

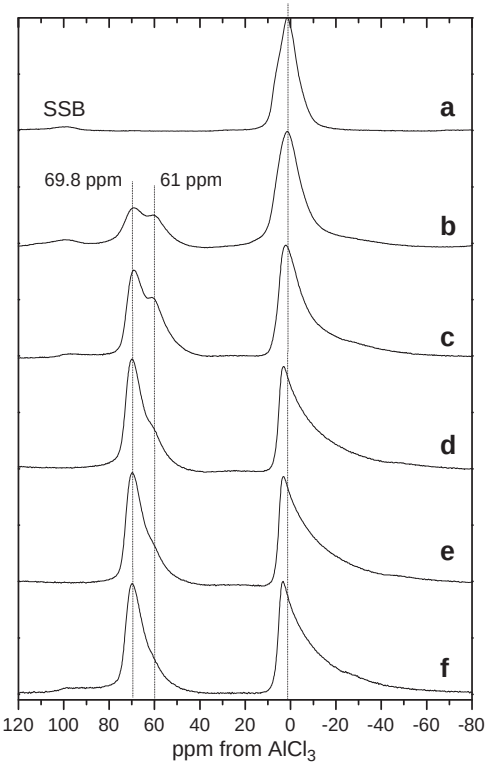

Fig. 2. ^{27}Al MAS NMR spectra of kaolinite before (a) and after hydrothermal reaction in 2.85 M KOH solution at 300 °C and 500 bar (b), 1000 bar (c), 1500 bar (d), 2000 bar (e) and 3000 bar (f). SSB = Spinning Side Band.

dehydrated interlayer K^+ ions. As pressure increased, the XRD patterns showed a notable increase of the intensity of the muscovite/illite reflexions, concomitant with the decreasing intensity of kaolinite reflections. At P≥1500 bar muscovite/illite appeared as the unique crystalline phase. The position of the 060 reflection shifted from 1.488 Å for kaolinite to 1.502 Å for muscovite/illite. The reflection at 4.11 Å (21.66°2θ in Fig. 1) indicated that the mica polytype formed was 1*M* at any pressure value. Examination of the XRD patterns reported by Huang (1993), who obtained muscovite/illite at 500 bar in KOH solution indicated the formation of the same polytype. Bentabol et al. (2003a), however, obtained a mixture of 1*M* and $2M_1$ polytypes in their experiments at lower pressure (~85 bar, which is the water vapour pressure controlling their experiments at 300 °C). Given that the results of the present study indicated that pressure does not influence the mica polytype formed, at least at *P*>500 bar, the formation of the second polytype at 300 °C in Bentabol et al. (2003a) could be favoured by the presence of other cations like Na^+ and Mg^{2+} in the system.

3.2. ^{27}Al MAS NMR spectroscopy study

The ^{27}Al MAS NMR spectra of the reaction products of kaolinite reacted for 12 h at 300 °C and increasing pressures are shown in Fig. 2. The spectrum of the starting kaolinite was also included. The spectrum of the unreacted kaolinite consisted of a signal centred at 1.5 ppm corresponding to the aluminium present in the octahedral sheet of the clay mineral (Müller et al., 1981). The shoulder on the high frequency side was explained as due to the effect of an electric field gradient at the quadrupolar aluminium nucleus (Meinhold et al., 1985). The asymmetry was also assigned by Hayashi et al. (1992) to

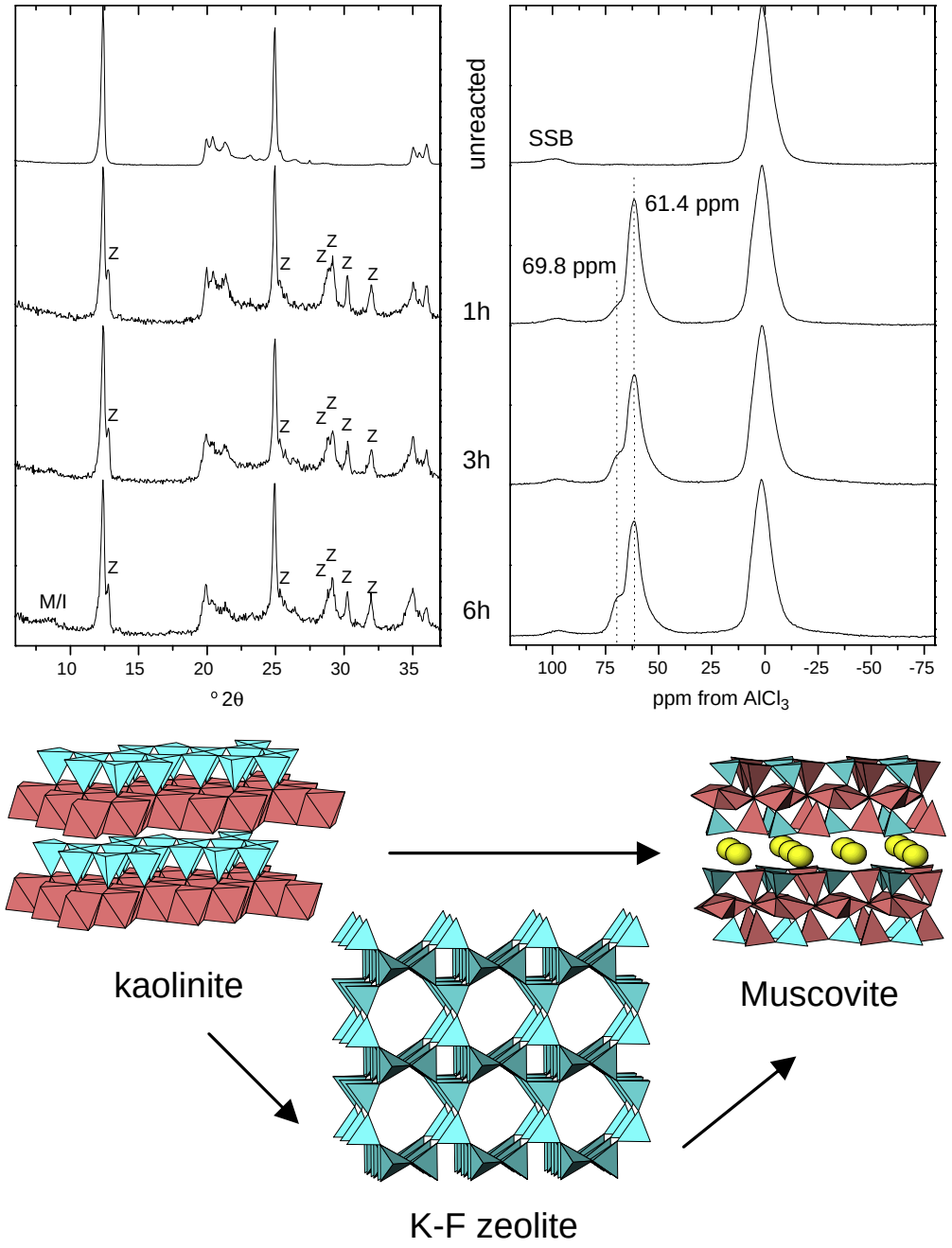

Fig. 3. XRD patterns (top left) and ^{27}Al MAS NMR spectra (top right) of kaolinite before and after hydrothermal reaction in 2.85 M KOH solution at 300 °C and 1000 bar for 1, 3 and 6 h. M/I: muscovite/illite. Z: K–F zeolite. SSB = Spinning Side Band. Bottom: Polyhedral representations of the crystal structures of kaolinite, muscovite and K–F zeolite.

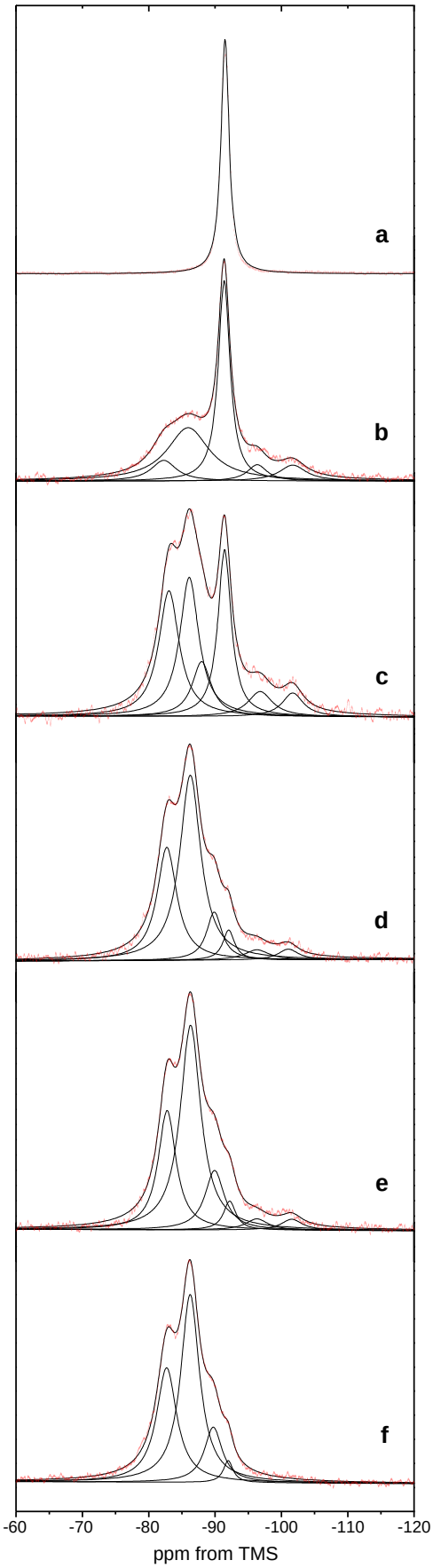

Fig. 4. ^{29}Si MAS NMR spectra of kaolinite before (a) and after hydrothermal reaction in 2.85 M KOH solution at 300 °C and 500 bar (b), 1000 bar (c), 1500 bar (d), 2000 bar (e) and 3000 bar (f). Crosses: Experimental. Continuous: Fit.

the presence of two aluminium sites in the octahedral sheet of the kaolinite structure, although Massiot et al. (1995), using two different magnets (7.0 T and 8.4 T), were unable to discriminate between the two types of ^{VI}Al sites. When kaolinite was submitted to the hydrothermal reaction at 300 °C and 500 bar (Fig. 2b), a new band with two maxima at ~61 and 69.8 ppm was observed in the frequency range corresponding to ^{IV}Al nuclei. At 1000 bar, the ^{IV}Al band intensity increased notably with respect to the intensity of the ^{VI}Al resonance. Subsequent reactions progressively decreased the signal at ~61 ppm and, eventually, a unique signal at 69.8 ppm was observed when the sample was reacted at 3000 bar. On the other hand, the signal corresponding to ^{VI}Al became more asymmetric with increasing pressure as a result of the quadrupolar interaction of the nucleus with the surrounding electric field gradient. This latter signal shifted slightly towards higher frequency values, showing the maximum at 3.4 ppm in the sample reacted at 3000 bar, to be compared to 1.5 ppm for the starting kaolinite.

According to the XRD data, the spectra of all the reaction products should show ^{27}Al resonances corresponding to muscovite/illite while those of samples reacted at 500 and 1000 bar, should also contain the ^{VI}Al signal of kaolinite. Sanz and Serratosa (1984) reported ^{IV}Al in pure muscovite at ~67 ppm and ^{VI}Al, at 1.5 ppm. Therefore, the high frequency ^{27}Al NMR resonance present in all the spectra at 69.8 ppm can be assigned to Al in the tetrahedral sheet of the muscovite/illite phase formed as a consequence of the reaction. The assignation of the ^{27}Al signal at ~61 ppm, clearly shown in the spectra of the samples reacted at 500 and 1000 bar, was not straightforward. In a previous study (Mantovani et al., 2009), the transformation of kaolinite into muscovite/illite was analysed at 300 °C and 500 bar with increasing reaction time. The XRD patterns showed a direct transformation of kaolinite into muscovite/illite while the ^{27}Al MAS NMR spectra showed the presence of a signal at ~60 ppm that was tentatively assigned to an intermediate phase representing a partially transformed kaolinite structure containing small amounts of ^{IV}Al. In order to look for a direct evidence of such phase, kaolinite was submitted to hydrothermal reactions in KOH solution at 300 °C and 1000 bar for 1, 3 and 6 h.

3.3. The secondary phase

The XRD patterns of the products of the hydrothermal reaction of kaolinite in KOH solution at 300 °C and 1000 bar for 1, 3 and 6 h are shown in Fig. 3 on the left. All three patterns showed a well resolved series of reflections of K–F zeolite ($KAlSiO_4 \cdot 1.5\ H_2O$, PDF 38-0216, marked with Z in the Figure). The pattern after 3 h reaction also showed the presence of a broad reflection of muscovite/illite at

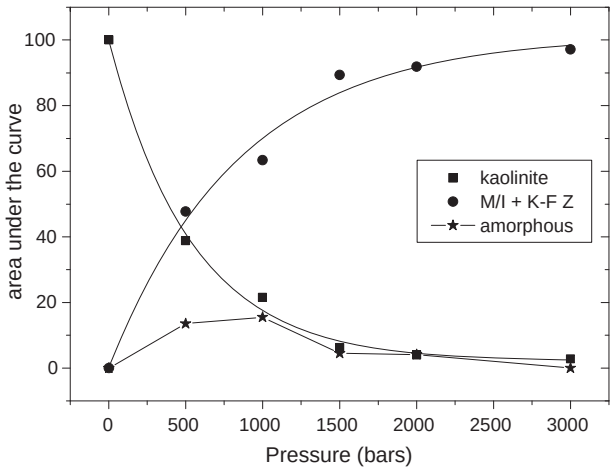

Fig. 5. Area under the curve (proportional to the number of Si nuclei) obtained from the fitting of the ^{29}Si MAS NMR spectra to the different contributions of Si environments for kaolinite, muscovite/illite, K–F zeolite and Si-containing amorphous phase.

8.7° 2θ, which increased in intensity with time. The typical reflections of kaolinite were still present after 6 h reaction. The corresponding ^{27}Al MAS NMR spectra are shown in Fig. 3 on the right. The spectra profile was similar to those in Fig. 2. At short reaction times, a new prominent signal was observed at 61.4 ppm that should correspond, according to the XRD data, to ^{IV}Al in the K–F zeolite. The intensity of the shoulder at higher frequency values increased with increasing reaction time and can be assigned to ^{IV}Al of muscovite/illite.

In view of these results, the ^{27}Al signals at ~61 ppm observed in the spectra of Fig. 2 must correspond to ^{VI}Al in K–F zeolite nuclei with a coherent diffraction domain size not large as to be detected by XRD. The results suggest, therefore, that kaolinite transformed into muscovite/illite, with the formation of K–F zeolite as a secondary metastable phase, which eventually transformed to muscovite/illite. Formation of zeolites during kaolinite illitization was reported by Bentabol et al. (2003a, 2006). Bauer et al. (1998), using low temperatures (35 °C and 80 °C) observed, however, direct transformation of kaolinite into illite, followed by KI-zeolite, phillipsite and K-feldspar when long reaction times (up to 150 days) were used. On the other hand, Huang (1993), in his study of illitization of kaolinite in KOH solution at 500 bar (very similar to the conditions used in our experiments), reported direct transformation of kaolinite into muscovite/illite, as observed by XRD. Given the results of the present study, it is likely that K–F zeolite nuclei were also present in his reaction products. Considerable structural changes are expected for the formation of zeolite from kaolinite, because it implies increasing

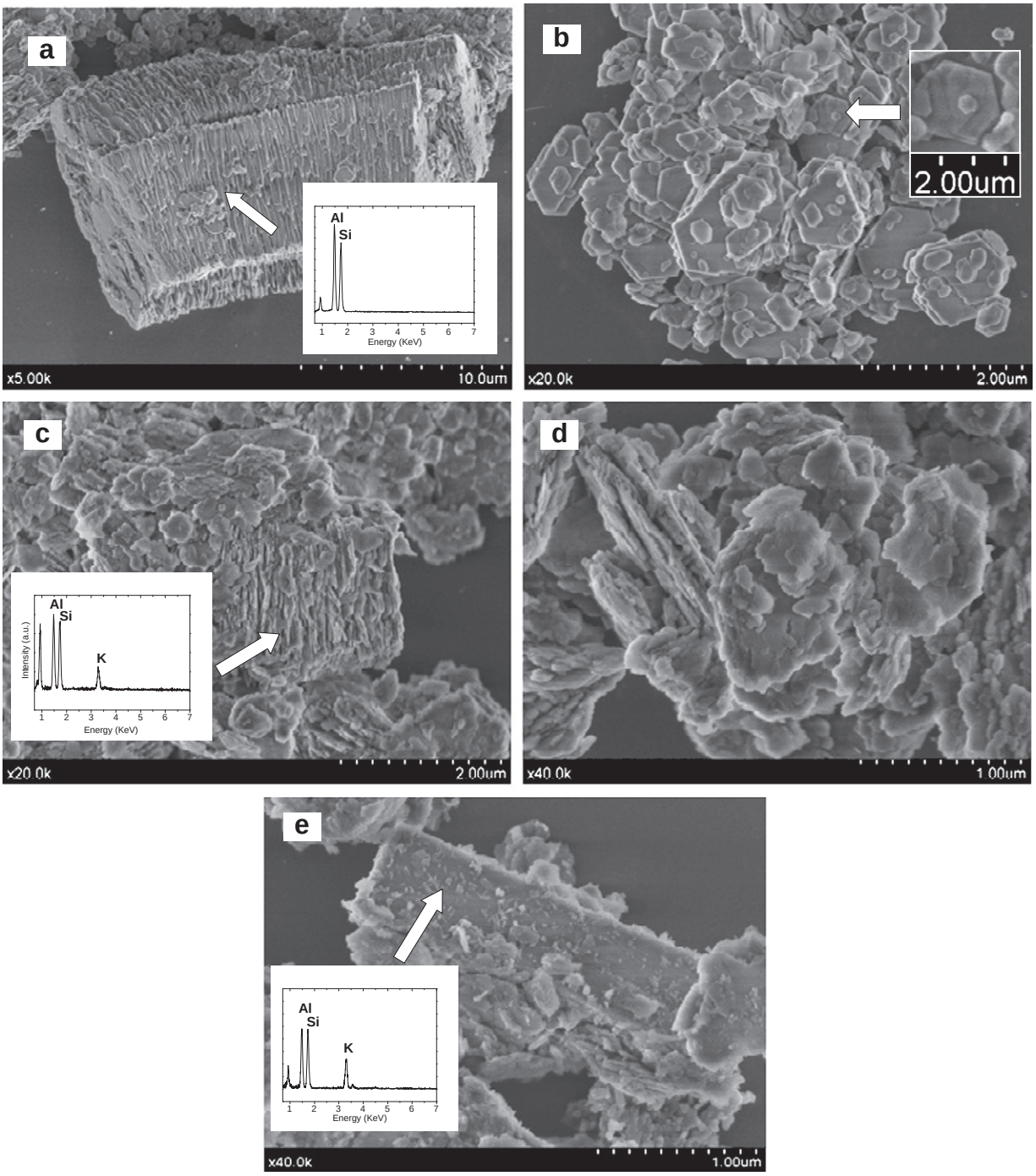

Fig. 6. Scanning electron microscope images of starting kaolinite (a and b), illite-muscovite obtained after hydrothermal reaction of kaolinite at 3000 bar (c and d) and a prismatic crystal of K–F zeolite in the product of hydrothermal reaction of kaolinite at 1000 bar for 3 h (e).

the condensation of Si tetrahedra (Q^3–Si to Q^4–Si), to transform a layered silicate to a tectosilicate and again decreasing from Q^4–Si to Q^3–Si to form muscovite/illite from K–F zeolite (Fig. 3, bottom).

3.4. Semiquantitative study of the illitization of kaolinite

The ^{29}Si MAS NMR spectra of kaolinite before and after the hydrothermal reaction in KOH solution at 300 °C for 12 h with increasing pressure are shown in Fig. 4. The starting material displayed a ^{29}Si spectrum consisting in a single symmetric signal at −91.5 ppm, corresponding to Q^3(0Al) units in the tetrahedral sheet of kaolinite (Kinsey et al., 1985). The hydrothermal reaction at 500 bar caused the appearance of a broad contribution on the high frequency side of the kaolinite resonance. The broad band is compatible with Si in muscovite/illite (expected at −89.5 ppm, −86.5 ppm and −83.0 ppm for Q^3(0Al), Q^3(1Al) and Q^3(2Al), respectively; (Weiss et al., 1987)) and K–F zeolite (expected a −85.6 ppm; (Engelhardt and Michel, 1987)). The intensity of the broad contribution increased as the kaolinite signal decreased with increasing run pressure. Attempts to decompose the spectra into five different contributions (three of muscovite/illite, one of K–F zeolite and one of kaolinite) were unsuccessful because of the proximity of the K–F zeolite signal to the one corresponding to Q^3(1Al) environment in muscovite/illite. These two signals were considered as a single one for the fittings and, eventually, only the content of Si nuclei in muscovite/illite + K–F zeolite could be obtained. An additional low intensity signal at ~ −100 ppm was necessary for a correct fitting of the low frequency region of the spectra. This signal could be produced by Q^4 units in an amorphous Si-containing phase not detectable by diffraction. Fig. 5 shows the evolution of the different Si environments with pressure. The signal of kaolinite decreased exponentially while that of muscovite/illite + K–F zeolite increased sharply at low pressure values and reached a plateau at P≥1500 bar. The Si-containing amorphous phase only appeared at low pressures and transformed eventually to muscovite/illite.

3.5. Morphology of the particles

Fig. 6a and b are SEM images of the starting kaolinite. Fig. 6a shows well-defined kaolinite books. The pseudo-hexagonal morphology of the particles, with clean edges, is observed in Fig. 6b. The EDX spectrum (inset of Fig. 6a) was in agreement with the chemical formula of the KGa-1b kaolinite. Fig. 6c and d are SEM images of muscovite/illite particles obtained after hydrothermal reaction of kaolinite at 300 °C and 3000 bar for 12 h. Fig. 6c displays aggregates of muscovite/illite particles that keep the book morphology of the unreacted kaolinite particles. The EDX spectrum (inset of Fig. 6c) indicated the incorporation of K^+ ions into the layered structure. The muscovite/illite particles showed very irregular edges (Fig. 6d). Finally, Fig. 6e is a SEM micrograph of a well-defined prismatic crystal corresponding to the K–F zeolite formed after 3 h reaction at 300 °C 1000 bar. The EDX analysis showed the presence of Si, Al, and K lines characteristic of this K–F zeolite. It was not possible to find this type of particles in any other sample reacted at 300 °C for 12 h with increasing pressure.

4. Conclusions

Muscovite/illite formed from kaolinite at the lowest pressure used in this study (i.e. 500 bar), with muscovite/illite as the unique stable phase at P≥1500 bar. Whilst XRD indicated a direct transformation of kaolinite into muscovite/illite, ^{27}Al MAS NMR results showed the development of a secondary metastable phase, K–F zeolite, which formed at 500 bar and progressively decreased with increasing pressure. An additional Si-containing amorphous phase was revealed by the ^{29}Si MAS NMR spectra of the samples reacted at the lower pressures. This study shows the importance of using techniques that inform on the local ordering of the atoms to detect the incipient formation of phases invisible to long range order techniques.

Acknowledgements

We are gratefully acknowledged to M. Carmen Jiménez for help with SEM. Bayerisches Geoinstitut is acknowledged for use of its Hydrothermal Lab. Supported by European Union VI Framework Programme as an HRM Activity (Contract number MRTN-CT-2006-035957), DGICYT (Project no. CTQ2007-63297) and Junta de Andalucía (Excellence Project P06-FQM-02179).

References

Bauer, A., Velde, B., Berger, G., 1998. Kaolinite transformation in high molar KOH solutions. Appl. Geochem. 13, 619–629.
Bailey, S.W., 1984. Classification and Structures of Micas. In: Bailey, S.W. (Ed.), Micas, Reviews in Mineralogy, vol 13. Mineralogical Society of America, Washington, D.C, pp. 1–12.
Bentabol, M., Ruiz Cruz, M.D., Huertas, F.J., Linares, J., 2003a. Hydrothermal transformation of kaolinite to illite at 200 and 300 °C. Clay Miner. 38, 161–172.
Bentabol, M., Ruiz Cruz, M.D., Huertas, F.J., Linares, J., 2003b. Characterization of the expandable clays formed from kaolinite at 200 °C. Clay Miner. 38, 445–458.
Bentabol, M., Ruiz Cruz, M.D., Huertas, F.J., Linares, J., 2006. Chemical and structural variablity of illitic phases formed from kaolinite in hydrothermal conditions. Appl. Clay Sci. 32, 111–124.
Bjorlikke, K., 1980. Clastic diagenesis and basin evolution. Revista del Instituto de Investigaciones Geológicas, Diputación Provincial, Universidad de Barcelona 34, 21–44.
Chermak, J.A., Rimstidt, J.D., 1990. The hydrothermal transformation rate of kaolinite to muscovite/ilite. Geochim. Cosmochim. Acta 54, 2979–2990.
De Almeida M.L., 1999. Illitisasion des minéraux argileux du groupe kaolin dans le champs pétrolier de Rind Norvège. Doctoral Thesis, Univ. Poitiers, France.
Dutta, P.K., Suttner, L.J., 1986. Alluvial sandstone composition and paleoclimate. II. authigenic mineralogy. J. Sed. Petrol. 56, 346–358.
Engelhardt, G., Michel, D., 1987. High Resolution Solid State NMR of Silicates and Zeolites. John Wiley and Sons, New York.
Grim, R.E., 1968. Clay Mineralogy, McGraw-Hill Book Company, (Ed.), New York.
Hancock, N.J., Taylor, A.M., 1978. Clay minerals diagenesis and oil migration in the Middle Jurassic Brent Sand Formation. J. Geol. Soc. 135, 69–72.
Hayashi, S., Ueda, T., Hayamizu, K., Akiba, E., 1992. NMR study of kaolinite. 1. ^{29}Si, ^{27}Al and ^{1}H Spectra. J. Phys. Chem. 26, 10928–10933.
Huang, W.L., 1993. The formation of illitic clays form kaolinite in KOH solution from 225 °C to 350 °C. Clays Clay Miner. 41, 645–654.
Kinsey, R.A., Kirkpatrick, R.J., Hower, J., Smith, K.A., Oldfield, E., 1985. High-resolution ^{27}Al and ^{29}Si nuclear magnetic-resonance spectroscopic study of layer silicates, including clay-minerals. Am. Mineral. 70, 537–548.
Kisch, H.J., 1983. Mineralogy and petrology of burial diagenesis (burial metamorphism) and incipient metamorphism in clastic rocks. In: Larsen, G., Chilanger, G.V. (Eds.), Diagenesis in Sedimentary Rocks, vol. 2. Elsevier, Amsterdam, pp. 289–493.
Mantovani, M., Escudero, A., Becerro, A.I., 2009. Application of ^{29}Si and ^{27}Al MAS NMR spectroscopy to the study of the reaction mechanism of kaolinite to illite/muscovite. Clays Clay Miner. 57, 302–310.
Martín, D., Gómez Gras, D., Sanfeliu, T., Permanyer, A., Núñez, J.A., Parcerisa, D., 2006. Conditions of kaolin illitization in the Permo-Triassic sandstones from the SE Iberian Ranges. Spain. J. Geochem. Explor. 89, 263–266.
Massiot, D., Dion, P., Alcover, J.F., Berjaya, F., 1995. ^{27}Al and ^{29}Si MAS NMR Study of kaolinite thermal decomposition by controlled rate thermal analysis. J. Am. Ceram. Soc., 2940–2944.
Massiot, D., Fayon, F., Capron, M., King, I., Le Calvé, S., Alonso, B., Durand, J.O., Bujoli, B., Gan, Z., Hoatson, G., 2002. Modelling one- and two-dimensional solid state NMR spectra. Magn. Reson. Chem. 40, 70–76.
Meinhold, R.H., MacKenzie, J.D., Brown, I.W.M., 1985. Thermal reactions of kaolinite by solid state 27-Al and 29-Si NMR. J. Mater. Sci. Lett. 4, 163–166.
Müller, D., Gessner, W., Behrens, H.J., Scheller, G., 1981. Determination of the aluminum coordination in aluminum-oxygen compounds by solid-state high-resolution Al-27 NMR. Chem. Phys. Lett. 79, 59–62.
Pruett, R.J., Harold, L.W., 1993. Sampling and analysis of KGa-1B well-crystallized kaolin source clay. Clays Clay Miner. 41, 514–519.
Sanz, J., Serratosa, J.M., 1984. Si-29 and Al-27 High resolution MAS-NMR spectra of phyllosilicates. J. Am. Chem. Soc. 106, 4790–4793.
Seeman, U., 1979. Diagenetically formed interstitial clay minerals as a factor in Rotliegend sandstone reservoir quality in the North Sea. J. Petrol. Geol. 1, 55–62.
Sommer, F., 1978. Diagenesis of Jurassic sandstones in the Vicking Graben. J. Geol. Soc. London 125, 63–67.
Velde, B., 1965. Experimental determination of muscovite polymorph stabilities. Am. Mineral. 50, 436–449.
Weiss, C.A., Altaner, S.P., Kirkpatrick, R.J., 1987. High-resolution ^{29}Si NMR spectroscopy of 2:1 layer silicates: correlations among chemical shift, structural distortions, and chemical variations. Am. Mineral. 72, 935–942.